

Leveraging exploration in off-policy algorithms via normalizing flows

Bogdan Mazoure^{* 1 2}, Thang Doan^{* 3},
Audrey Durand^{1 2}, R Devon Hjelm^{2 7}, Joelle Pineau^{1 2 5}

¹School of Computer Science, McGill University

²Mila – Quebec Artificial Intelligence Institute

³Desautels Faculty of Management, McGill University

⁴Microsoft Research Montreal, ⁵Facebook AI Research

Abstract

Exploration is a crucial component for discovering approximately optimal policies in most high-dimensional reinforcement learning (RL) settings with sparse rewards. Approaches such as neural density models and continuous exploration (e.g., Go-Explore) have been instrumental in recent advances. Soft actor-critic (SAC) is a method for improving exploration that aims to combine off-policy updates while maximizing the policy entropy. We extend SAC to a richer class of probability distributions through normalizing flows, which we show improves performance in exploration, sample complexity, and convergence. Finally, we show that not only the normalizing flow policy outperforms SAC on MuJoCo domains, it is also significantly lighter, using as low as 5.6% of the original network’s parameters for similar performance.

1 Introduction

The importance of exploration in reinforcement learning (RL) cannot be overstated, as training agents to directly maximize the expected return in challenging environments will likely become trapped in sub-optimal solutions. Difficulties in finding the optimal policy are characterized by two hard problems: sparse rewards (Pathak et al., 2017) and deceptive rewards (Ecoffet et al., 2019). For example, the first reward in the well-known Montezuma’s Revenge game is encountered after 100 environment steps (a search space roughly of size 100^{18} , e.g., see Aytar et al., 2018), which is unsolvable without structured exploration strategies.

In order to address the problem of sparse rewards, exploration-based algorithms introduce a variety of components to improve exploration. Bellemare et al. (2016); Tang et al. (2016) maintain state visitation frequencies which act as intrinsic motivation. Other works (Henderson et al., 2017; Osband et al., 2016) model uncertainty by estimating the state-action value function, thus simultaneously keeping track of multiple promising solutions. Bellemare, Dabney, and Munos (2017) use a categorical distribution to keep track of the random returns to bolster exploratory actions. In a similar vein, Doan, Mazoure, and Lyle (2018) rely on a generative model to learn the distribution of state-action values. In that case, approximating the return density with a generator allows to

cover a wide range of sub-optimal moves and plays a role similar to that of an exploration strategy.

Although count-based methods (Bellemare et al., 2016; Tang et al., 2016) have strong theoretical guarantees, they have traditionally been used to solve tasks with sparse rewards. On the other hand, deceptive environments which trap agents within local minima are just as tricky to solve. For instance, some navigation and locomotion tasks such as biped walking possess deceptive reward regions which attract the agent into low reward regions (Conti et al., 2017). A straightforward approach to boosting exploration in challenging environments consists in increasing the capacity of the policy such that it is able to capture a more refined landscape. Indeed, a more expressive policy allows to keep track of local optima (Haarnoja et al., 2017) and hence are at lower risk to fall into them.

Previous results (Rezende and Mohamed, 2015) suggest that a complex and potentially multi-modal distribution can be decomposed into a sequence of invertible transformations denoted *normalizing flows*, applied on the original (simple) density. This approach has been used in the off-policy setting and positioned as an effective exploration technique (Tang and Agrawal, 2018).

In this work, we show that normalizing flows-based policies can form a natural extension to the Soft Actor-Critic (SAC) algorithm (Haarnoja et al., 2018), which we call SAC-NF. We show empirically that this simple extension significantly improves upon the already high exploration rate of SAC and achieves better convergence properties as well as better empirical performance. Last but not least, the class of policies that we propose requires significantly less parameters than its baseline counterpart, while also improving on the original results. Finally, we assess the performance of both SAC and SAC-NF across a variety of benchmark continuous control tasks from OpenAI Gym using the MuJoCo simulator (Todorov, Erez, and Tassa, 2012).

This paper is organized as follows. Section 2 first reviews previous literature relevant to our work. Section 3 provides an overview of background material, before introducing the proposed SAC-NF approach in Section 4. Section 5 first shows an empirical analysis of SAC-NF expressivity through toy experiments before comparing against SAC on Mujoco benchmark environments. Section 6 finally provides conclusions and future directions.

Preprint. Work in progress.

* Equal contribution.

2 Related Work

Off-policy RL The idea behind off-policy strategies in RL is to collect samples under some behaviour policy and use them to train a target policy. Off-policy algorithms are known to train faster than their on-policy counterparts, but at the cost of higher variance and instability (Lillicrap et al., 2016). Among this family, actor critic (AC) strategies have shown great success for solving continuous control tasks. In between value-based and policy-based approaches, an AC algorithm trains an *actor* (policy-based) using guidance from a *critic* (value-based). Two major AC algorithms, SAC (Haarnoja et al., 2018) and TD3 (Fujimoto, van Hoof, and Meger, 2018), have shown a large performance improvement over previous off-policy algorithms such as DDPG (Lillicrap et al., 2016) or A3C (Mnih et al., 2016). While TD3 does so by maintaining a second critic network to alleviate the overestimation bias, SAC enforces exploration by adding an entropy regularization term.

Density estimation for better exploration Using powerful density estimators to model state-action values with the aim to improve exploration generalization has been a long-standing practice in RL. For instance, Henderson et al. (2017) use dropout approximation (Gal and Ghahramani, 2016) within a Bayesian network and show improvement on stability and performance of policy gradient methods. Osband et al. (2016) rather rely on an ensemble of neural networks to estimate the uncertainty in the prediction of the value function, allowing to reduce learning times while improving performance. Finally, Doan, Mazouze, and Lyle (2018) consider generative adversarial networks (Goodfellow et al., 2014) to model the distribution of random state-value functions. The current work considers a different approach based on normalizing flows for density estimation.

Normalizing flows Flow-based generative models have proven to be powerful density approximators (Rezende and Mohamed, 2015). The idea is to relate an initial noise density distribution to a posterior distribution using a sequence of invertible transformations, parametrized by a neural network and having desirable properties. For example, invertible autoregressive flows (IAF) are characterized by a simple-to-compute Jacobian (Kingma, Salimans, and Welling, 2016). In their original formulation, IAF layers allow to learn location-scale invariant (i.e. affine) transformations of the simple initial noise density. Normalizing flows have been used previously in the on-policy RL setting where IAF extends a base policy found by TRPO (Tang and Agrawal, 2018). In this work, we tackle the off-policy learning setting, and we focus on planar and radial flows, which are known to provide a good trade-off between function expressivity and time complexity (Rezende and Mohamed, 2015).

3 Background

In this section, we review the formal setting of RL in a Markov decision process (MDP), the policy optimization approaches considered in this paper, and the general framework of normalizing flows, which will be used to improve exploration in Section 4.

3.1 Markov Decision Process

A discrete-time, finite-horizon, MDP (Bellman, 1957; Puterman, 2014) is described by a state space \mathcal{S} (either discrete or continuous), an action space \mathcal{A} (either discrete or continuous), a transition function $\mathcal{P} : \mathcal{S} \times \mathcal{A} \times \mathcal{S} \mapsto \mathbb{R}^+$, and a reward function $r : \mathcal{S} \times \mathcal{A} \mapsto \mathbb{R}$. MDPs are useful for modelling sequential decision-making problems. On each round t , an agent interacting with this MDP observes the current state $s_t \in \mathcal{S}$, selects an action $a_t \in \mathcal{A}$, and observes a reward $r_t = r(s_t, a_t) \in \mathbb{R}$ upon transitioning to a new state $s_{t+1} \sim \mathcal{P}(s_t, a_t)$. Let $\gamma \in [0, 1]$ be a discount factor. The goal of an agent evolving in a discounted MDP is to learn a policy $\pi : \mathcal{S} \times \mathcal{A} \mapsto [0, 1]$ such as taking action $a_t \sim \pi(\cdot | s_t)$ would maximize the expected sum of discounted returns,

$$V^\pi(s) = \mathbb{E}_\pi \left[\sum_{t=0}^{\infty} \gamma^t r_t | s_0 = s \right].$$

The corresponding state-action value function can be written as the expected discounted rewards from taking action a in state s , that is

$$Q_t^\pi(s, a) = \mathbb{E}_\pi \left[\sum_{i=t}^{\infty} \gamma^{i-t} r(s_i, a_i) | s_t = s, a_t = a \right].$$

We use ρ_π to denote the trajectory distribution induced by following policy π . If \mathcal{S} or \mathcal{A} are vector spaces, action and space vectors are respectively denoted by \mathbf{a} and \mathbf{s} .

3.2 Policy Optimization

Policy gradient methods (Sutton et al., 1999) are a class of algorithms for learning RL policies, relying on stochastic gradient descent to optimize the discounted return through gradient steps on the policy parameters. While this has been addressed in the on-policy setting, for instance by restricting changes in the policy to be constrained within a trust region (Schulman et al., 2015), on-policy strategies suffer from a high sample complexity. On the other hand, their off-policy alternatives (Lillicrap et al., 2016) are subject to instability, especially in continuous state and action spaces. Recently, SAC (Haarnoja et al., 2018) has been shown to mitigate this by optimizing a maximum entropy policy objective function:

$$J(\pi) = \sum_{t=0}^T \mathbb{E}_{(s_t, a_t) \sim \rho_\pi} [r(s_t, a_t) + \alpha H(\pi(\cdot | s_t))], \quad (1)$$

where $H(\pi(\cdot | s_t))$ is the entropy of the policy and α is the importance given to the entropy regularizer. The entropy term allows to prevent mode collapse on the highest reward and to maintain the exploration rate above some threshold.

3.3 Normalizing Flows

Normalizing flows are useful to generate samples from complex probability distributions (Rezende and Mohamed, 2015). More specifically, they provide a general framework for extending the change of variable theorem for density functions to a sequence of d -dimensional real random variables $\{\mathbf{z}_i\}_{i=0}^N$. The initial random variable \mathbf{z}_0 has density function q_0 and is linked to the final output of the flow \mathbf{z}_N through

a sequence of invertible, smooth mappings $\{f_i\}_{i=1}^N$ called *normalizing flows* of length N , such that

$$\log q_N(\mathbf{z}_N) = \log q_0(\mathbf{z}_0) - \sum_{i=1}^N \log \left| \det \frac{\partial f_i(\mathbf{z}_{i-1})}{\partial \mathbf{z}_{i-1}} \right|. \quad (2)$$

Specific forms of the mapping can be selected based on desired properties: highly expressive and sometimes invertible maps (Rezende and Mohamed, 2015), always invertible affine transformations (Kingma, Salimans, and Welling, 2016), volume-preserving and orthogonal transformations (Tomczak and Welling, 2016) or always invertible and highly expressive networks (Huang et al., 2018). For example, the family of radial contractions around a point $\mathbf{z}_0 \in \mathbb{R}^d$ defined as (Rezende and Mohamed, 2015):

$$f(\mathbf{z}) = \mathbf{z} + \frac{\beta}{\alpha + \|\mathbf{z} - \mathbf{z}_0\|_2} (\mathbf{z} - \mathbf{z}_0) \quad (3)$$

are highly expressive (i.e. represent a wide set of distributions) and yet very light (parameter-wise), in addition to enjoying a closed-form determinant

$$\left| \det \frac{\partial f(\mathbf{z})}{\partial \mathbf{z}} \right| = [1 + \beta h(\alpha, r)]^{d-1} \cdot [1 + \beta h(\alpha, r) + \beta h'(\alpha, r)r] \quad (4)$$

for $r = \|\mathbf{z} - \mathbf{z}_0\|_2$, $h(\alpha, r) = \frac{1}{\alpha + r}$, $\alpha \in \mathbb{R}^+$ and $\beta \in \mathbb{R}$. The family of radial maps defined above allows to approximate the target posterior through a sequence of concentric expansions of arbitrary width and centered around a learnable point \mathbf{z}_0 . In order to guarantee that the flow is invertible, it is sufficient to pick $\beta \geq -\alpha$. As pointed out by Kingma, Salimans, and Welling (2016), radial and planar flows have an advantage in lower dimensions (up to a few hundreds) since they require a low number of parameters while being highly expressive.

4 Augmenting SAC with Normalizing Flows

We now propose a flow-based formulation of the off-policy maximum entropy RL objective (Eq. 1) and argue that SAC is a special case of the resulting approach, called SAC-NF, where the normalizing flow layers are over-regularized.

4.1 Entropy maximization in RL

Recall that the SAC algorithm (Haarnoja et al., 2018) finds the information projection of the Boltzmann Q-function onto the set of diagonal Gaussian policies Π , such that an update in the policy improvement step is given by:

$$\pi_{\text{new}} = \arg \min_{\pi' \in \Pi} \text{D}_{\text{KL}} \left(\pi'(\cdot | \mathbf{s}_t) \left\| \frac{\exp(\frac{1}{\alpha} Q^{\pi_{\text{old}}}(\mathbf{s}_t, \cdot))}{Z^{\pi_{\text{old}}}(\mathbf{s}_t)} \right. \right), \quad (5)$$

where D_{KL} denotes the Kullback-Leibler divergence and $\alpha \in (0, 1)$ controls the temperature, i.e. the peakedness of the distribution. Equivalently, the objective can be reformulated as a maximum entropy RL task:

$$\begin{aligned} \pi_{\text{new}} &= \arg \max_{\pi' \in \Pi} \mathbb{E}_{(\mathbf{s}_t, \mathbf{a}_t) \sim \rho_{\pi'}} [r(\mathbf{s}_t, \mathbf{a}_t)] \\ \text{such that} & \quad \mathbb{E}_{\mathbf{s}_t \sim \rho_{\pi'}} [H(\pi'(\cdot | \mathbf{s}_t))] \text{ is maximized,} \end{aligned} \quad (6)$$

where the differential entropy of the policy is denoted point-wise as $H(\pi(\cdot | \mathbf{s}_t)) = \mathbb{E}_{\pi} [\log \pi]$ for every state \mathbf{s}_t in trajectory $\rho_{\pi'}$. If $\pi(\cdot | \mathbf{s}_t) \sim \mathcal{N}(\mu, \Sigma)$ for some mean vector μ and covariance matrix Σ in a fixed-dimensional space, then $H(\pi(\cdot | \mathbf{s}_t)) \propto \log \det(\Sigma)$. When Σ is diagonal, then the entropy is directly proportional to the sum of log-variances. The task tackled by SAC can hence be re-formulated as maximizing expected discounted rewards while keeping the volume of the policy at a certain level. Doing so keeps exploration active and prevents mode collapse on the highest reward.

The policy is updated using Eq. 5, while the state-action value function is trained using soft updates on the critic and state value functions. A major drawback of diagonal Gaussian policies lies in their symmetry: reaching global optima lying far away requires a large variance, but avoiding being stuck in suboptimal solutions requires a damped entropy in cases where local and global optima are close.

4.2 Exploration through normalizing flows

We propose a class of policies comprised of an initial noise sample \mathbf{a}_0 , a state-noise embedding $h_{\theta}(\mathbf{a}_0, \mathbf{s}_t)$ and of a normalizing flow $\{f_{\phi}\}_{i=1}^N$ of arbitrary length N parameterized by $\phi = \{\phi_i\}_{i=1}^N$. Sampling from the policy $\pi_{\phi, \theta}(\mathbf{a}_t | \mathbf{s}_t)$ can be described by the following set of equations:

$$\mathbf{a}_t = f_{\phi_N} \circ f_{\phi_{N-1}} \circ \dots \circ f_{\phi_1}(\mathbf{z}), \quad (7)$$

$$\mathbf{z} = h_{\theta}^j(\mathbf{a}_0, \mathbf{s}_t), \quad j = 1, 2, 3 \quad (8)$$

$$\mathbf{a}_0 \sim \mathcal{N}(0, \mathbf{I}), \quad (9)$$

where h_{θ}^j depends on the noise and the state. This deterministic mapping takes values from the set below to the action space

$$h^j(\mathbf{a}_0, \mathbf{s}_t) = \begin{cases} [\mathbf{a}_0, \mu(\mathbf{s}_t)] \mathbf{L}, & j = 1 \\ \mathbf{a}_0 \mathbf{L}(\mathbf{s}_t) + \mu(\mathbf{s}_t), & j = 2 \\ \mathbf{a}_0 \sigma \mathbf{I} + \mu(\mathbf{s}_t), & j = 3 \end{cases} \quad (10)$$

where $[\mathbf{a}, \mathbf{b}]$ denotes concatenation of vectors \mathbf{a} and \mathbf{b} . Intuitively, h^1 corresponds to a non-parametric generator network, while h^2 samples $\mathbf{z} \sim \mathcal{N}(\mu(\mathbf{s}_t), \mathbf{L}(\mathbf{s}_t) \mathbf{L}(\mathbf{s}_t)^{\top})$ following the reparametrization trick in variational Bayes (Kingma and Welling, 2014). Precisely, $\mu(\mathbf{s}_t) : \mathcal{S} \rightarrow \mathbb{R}^d$ is a state embedding function and $\mathbf{L}, \mathbf{L}(\mathbf{s}_t), \sigma \mathbf{I}$ plays the role of a covariance matrix. While in theory h^1 and h^3 are equivalent up to a multiplicative constant to sampling $\mathbf{z} \sim \mathcal{N}(\mu(\mathbf{s}_t), \mathbf{L} \mathbf{L}^{\top})$, in practice h^3 yields lower variance estimates.

In the limit, we can recover the original base policy through heavy regularization:

$$\lim_{\|\phi_1\|, \dots, \|\phi_N\| \rightarrow 0} \pi(\cdot | \mathbf{s}_t) \stackrel{d}{=} \mathcal{N}(\mu(\mathbf{s}_t), \mathbf{L} \mathbf{L}^{\top}) \quad (11)$$

for all states $\mathbf{s}_t \in \mathcal{S}$, implying that $\Pi \subseteq \Pi_{\text{NF}}$. When $j = 2$, a similar statement holds for \mathbf{L} replaced by $\mathbf{L}(\mathbf{s}_t)$ and by $\sigma \mathbf{I}$ when $j = 3$. By analogy with the SAC updates, SAC-NF searches the information projection of Q onto the feasible set of policies Π_{NF} by minimizing the negative variational lower bound w.r.t. parameters θ and ϕ , using samples from replay buffer \mathcal{D} :

$$\mathcal{L}_{\pi} = \mathbb{E}_{\mathbf{s}_t \sim \mathcal{D}} \left[\mathbb{E}_{\mathbf{a}_t \sim \pi} [\alpha \log \pi_{\theta, \phi}(\mathbf{a}_t | \mathbf{s}_t) - Q(\mathbf{s}_t, \mathbf{a}_t)] \right], \quad (12)$$

where the policy density is decomposed on a log scale

$$\log \pi(\mathbf{a}_t, \mathbf{s}_t) = \log q_0(\mathbf{a}_0) - \log |\det \mathbf{L}| - \sum_{i=1}^N \log \left| \det \frac{\partial f_i(\mathbf{a}_{i-1})}{\partial \mathbf{a}_{i-1}} \right|.$$

The term involving \mathbf{L} appears through chain rule or recalling the gradient of a multivariate normal density with respect to the Cholesky factor \mathbf{L} of its covariance. Note that for h^2 , it would be replaced by $\mathbf{L}(\mathbf{s}_t)$.

The (soft) state value function is parameterized by ν and defined exactly as for SAC:

$$V_\nu^\pi(\mathbf{s}_t) = \mathbb{E}_{\mathbf{a}_t \sim \pi} [Q(\mathbf{s}_t, \mathbf{a}_t) - \alpha \log \pi(\mathbf{a}_t | \mathbf{s}_t)]$$

and estimated by minimizing the mean squared error:

$$\mathcal{L}_V = \mathbb{E}_{\mathbf{s}_t \sim \mathcal{D}} \left[\frac{1}{2} \{V_\nu^\pi(\mathbf{s}_t) - \mathbb{E}_{\mathbf{a}_t \sim \pi} [Q(\mathbf{s}_t, \mathbf{a}_t) - \alpha \log \pi(\mathbf{a}_t | \mathbf{s}_t)]\}^2 \right].$$

Similarly, the state-action value function is parameterized by ω and learned using the standard temporal difference loss:

$$\mathcal{L}_Q = \mathbb{E}_{(\mathbf{s}_t, \mathbf{a}_t) \sim \mathcal{D}} \left[\frac{1}{2} \{Q_\omega(\mathbf{s}_t, \mathbf{a}_t) - r(\mathbf{s}_t, \mathbf{a}_t) + \gamma \mathbb{E}_{\mathbf{s}_{t+1} \sim \mathcal{D}} [V(\mathbf{s}_{t+1})]\}^2 \right].$$

In practice, we use m Monte-Carlo samples to approximate the gradient of each loss:

$$\nabla_\theta \hat{\mathcal{L}}_\pi \approx \frac{1}{m} \sum_{i=1}^m \nabla_\theta (\alpha \log \pi_{\theta, \phi}(\mathbf{a}_t | \mathbf{s}_i) - Q_\omega(\mathbf{s}_i, \mathbf{a}_t)). \quad (13)$$

Algorithm 1 outlines the proposed method: the major distinction from the original SAC is the additional gradient step on the normalizing flows layers while holding the base policy function h constant.

5 Experiments

This section addresses two major points: (1) it highlights the beneficial impact of NF on exploration through two toy examples and (2) it compares the proposed SAC-NF approach against SAC, i.e. the current state-of-the-art, on a set of continuous control tasks from MuJoCo (Todorov, Erez, and Tassa, 2012). For all experiments, we hold the entropy rate α constant at 0.2 for every environment except 0.05 for `Humanoid-v2` following the tuning reported by Haarnoja et al. (2018). Optimal values for SAC-NF are reported in the Appendix (Table 2).

5.1 Managing multi-modal policies

We first conduct a synthetic experiment to illustrate how the augmentation of a base policy with normalizing flows allows to represent multi-modal policies. We consider a navigation task environment with continuous state and action spaces consisting of four goal states symmetrically placed around

Algorithm 1 SAC-NF

Input: Mini-batch size m ; replay buffer \mathcal{D} ; number of epoch T ; learning rates $\alpha_\theta, \alpha_\phi, \alpha_\nu, \alpha_\omega$
Initialize value function network $V_\nu^\pi(\mathbf{s})$
Initialize critic network $Q_\omega^\pi(\mathbf{s}, \mathbf{a})$
Initialize policy network with weights $\pi_{\phi, \theta}(\mathbf{s})$
for epoch = 1, ..., T **do**
 $\mathbf{s} \leftarrow \mathbf{s}_0$
for t=0... **do**
 $\mathbf{a}_t \sim \pi(\cdot | \mathbf{s}_t)$
Observe $\mathbf{s}_{t+1} \sim P(\cdot | \mathbf{s}_t, \mathbf{a}_t)$ and get reward r_t
Store transition $(\mathbf{s}_t, \mathbf{a}_t, r_t, \mathbf{s}_{t+1})$ in \mathcal{D}
for each learning step **do**
{Update networks with m MC samples each}
 $\nu \leftarrow \nu - \alpha_\nu \nabla_\nu \hat{\mathcal{L}}_V$ {Update value function}
 $\omega \leftarrow \omega - \alpha_\omega \nabla_\omega \hat{\mathcal{L}}_Q$ {Update critic}
 $\theta \leftarrow \theta - \alpha_\theta \nabla_\theta \hat{\mathcal{L}}_\pi$ {Update base policy}
 $\phi \leftarrow \phi - \alpha_\phi \nabla_\phi \hat{\mathcal{L}}_\pi$ {Update NF layers}
end for
end for
end for

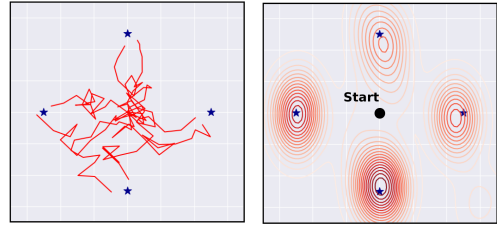


Figure 1: 4-goals navigation task outlining the ability of normalizing flows to learn multi-modal policies. The left subfigure shows some trajectories sampled from the SAC-NF agent. The right subfigure shows a KDE plot of terminal state visitations by the agent.

the origin. The agent starts at the origin and, on each time t , receives reward r_t corresponding to the Euclidean distance to the closest goal. We consider a SAC-NF agent (Algorithm 1 with mini-batch size $m = 256$, 4 flows and one hidden layer of 8 neurons), which can represent radial policies. The agent is trained over $T = 500$ epochs, each epoch consisting of 20 time steps.

Figure 1 displays some trajectories sampled by the SAC-NF agent along with the kernel density estimation (KDE) of terminal state visitations by the agent. Trajectories are obtained by sampling from respective policy distributions instead of taking the average action. We observe that the SAC-NF agent, following a flow-based policy, is able to successfully visit all four modes.

5.2 Robustness to confounding rewards

We now show through a environment with deceptive rewards that, unlike the Gaussian policy, radial policies are able to find the global optimal solution. We consider an environ-

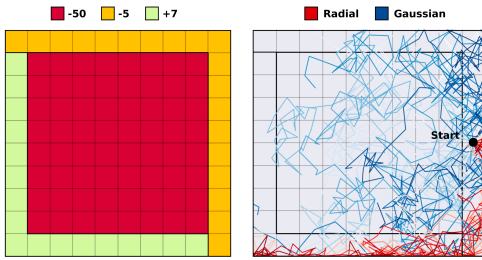


Figure 2: A deceptive reward environment where the high reward region is hidden behind a negative reward region (left subfigure). The right subfigure shows trajectories of Gaussian and radial agents. While the Gaussian policy is exploring vaguely the yellow region and falls into the pit, the normalizing flows policy manages to find the optimal region by going from the yellow to green zone.

ment composed of three reward areas: a locally optimal strip around the initial state, a global optimum on the opposing end of the room, separated by a pit of highly negative reward. The agent starts at the position $s_0 = (4.5, 0)$ and must navigate into the high rewards area without falling into the pit. On each time t , the agent receives the reward r_t associated to its current location s_t .

We compare the SAC-NF agent (Algorithm 1 with mini-batch size $m = 256$, 4 flows and one hidden layer of 8 neurons), which can represent radial policies, with a classical SAC agent (two hidden layers of 16 units) that models Gaussian policies. Both agents are trained over $T = 500$ epochs, each epoch consisting of 20 time steps.

Figure 2 displays the trajectories visited by both agents. This highlights the biggest weakness of diagonal Gaussian policies: the agent is unable to simultaneously reach the region of high rewards while avoiding the center of the room. In this case, lowering the entropy threshold will lead to the conservative behaviour of staying in the yellow zone; increasing the entropy leads the agent to die without reaching the goal. Breaking the symmetry of the policy by adding (in this case three) radial flows allows the agent to successfully reach the target area by walking along the safe path surrounding the room.

In the case of steep reward functions, where low rewards border on high rewards, symmetric distributions force the agent to explore into all possible directions. This leads the agent to sometimes attain the high reward region, but, more dangerously, falling into low reward areas with non-zero probability.

5.3 MuJoCo locomotion benchmarks

In this section, we compare our SAC-NF method against the SAC baseline on five continuous control tasks from the Mujoco suite (see Figure 3): Ant-v2, HalfCheetah-v2, Humanoid-v2, Hopper-v2 and Walker2d-v2.

The SAC-NF agent consists of one feedforward hidden layer of 256 units acting as state embedding, which is then followed by a normalizing flow of length $N \in \{3, 4, 5\}$. Details of the model can be found in table 2. For the SAC

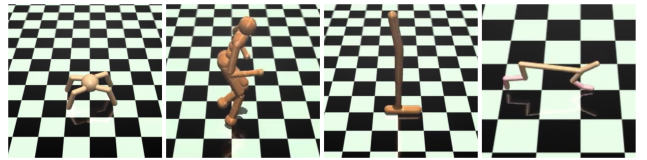


Figure 3: Illustration of each MuJoCo environment. From left to right: Ant, Humanoid, Hopper, HalfCheetah.

baseline, two hidden layers of 256 units are used. The critic and value function architectures are the same as in Haarnoja et al. (2018). All networks are trained with Adam optimizer (Kingma and Ba, 2015) with a learning rate of $3E^{-4}$.

Figure 4 displays the performance of both SAC and SAC-NF. Each curve is averaged over 5 random seeds (bold line) and one standard deviation confidence intervals are represented as shaded regions over 1 millions steps (or 2 million steps for Humanoid-v2). Every 10, 000 environment steps, we evaluate our policy 10 times and report the average. The best observed reward for each method can be found in Table 1. We observe that SAC-NF shows faster convergence, which translates into better sample efficiency, compared to the baseline. Indeed, SAC-NF takes advantage of the expressivity of normalizing flows to allow for better exploration and thus discover new policies. In particular, we notice that SAC-NF performs well on two challenging tasks Humanoid-v2 and Ant-v2 which are known to require hard exploration.

Table 1 not only shows better performance from SAC-NF in most of the environments, but also points out the reduction in the number of parameters for our policy architecture. For instance, on Hopper-v2, we could reduce up to by 95% the number of parameters (70, 406 parameters for SAC baseline versus 3, 914 for SAC-NF) and by 33% the number of parameters in Humanoid-v2, while performing at least as well as the baseline. Moreover, note that SAC-NF uses a lower entropy rate α than the baseline (0.05 versus 0.2), suggesting that unlike SAC which explicitly encourages exploratory actions, SAC-NF achieves it through fitting the Boltzmann Q-function.

	SAC	SAC-NF	$\frac{\#\{\text{SAC-NF}\}}{\#\{\text{SAC}\}}$
Ant-v2	3151 \pm 930	4071 \pm 341	$\approx 33\%$
HalfCheetah-v2	6609 \pm 1334	6504 \pm 524	$\approx 8.6\%$
Hopper-v2	2927 \pm 700	3039 \pm 698	$\approx 5.6\%$
Humanoid-v2	5320 \pm 275	5613 \pm 243	$\approx 62\%$
Walker2d-v2	3824 \pm 641	4210 \pm 353	$\approx 8.5\%$

Table 1: Maximal average return \pm one standard deviation across 5 random seeds. The last column represents the ratio of the numbers of parameters of the SAC-NF policy over the

SAC policy. A value lower than 100% means that the SAC-NF policy network has a lower number of parameters.

6 Conclusion

In this paper, we proposed a novel algorithm which combines the soft actor-critic updates together with a sequence

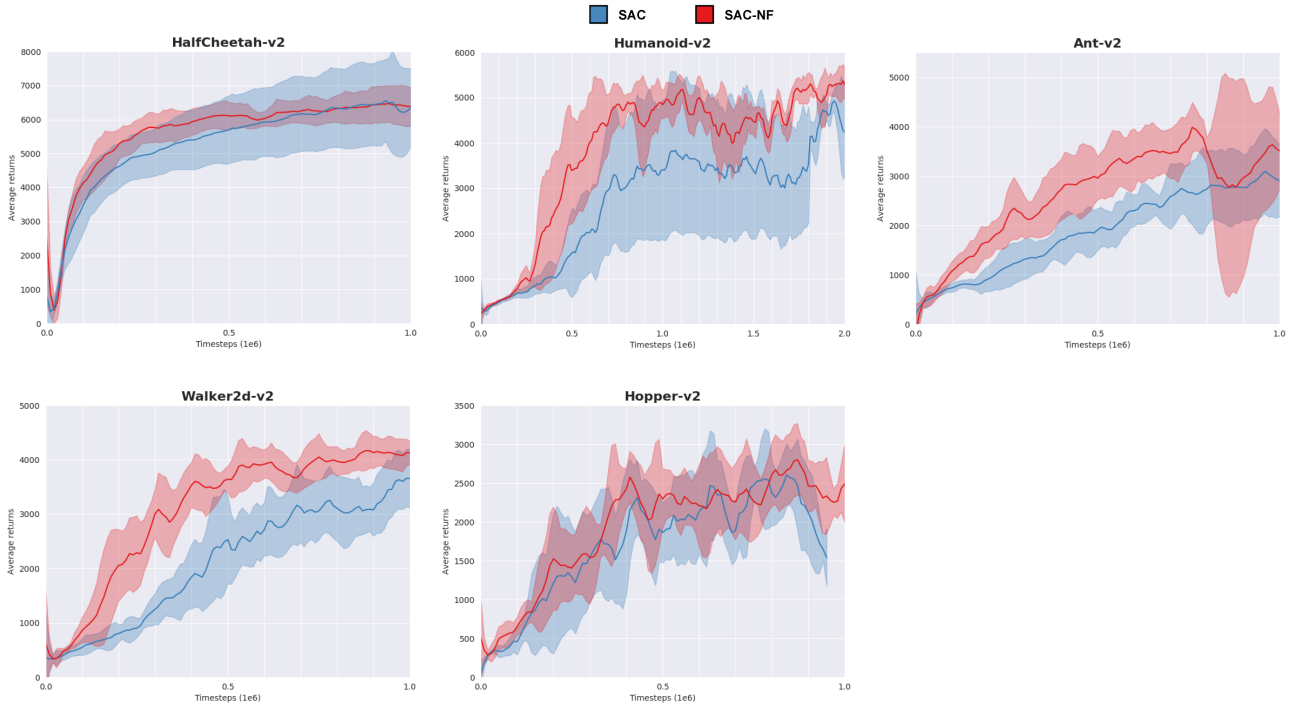


Figure 4: Performance of SAC-NF against SAC across 5 MuJoCo tasks (higher is better). Curves are averaged over 5 random seeds and then smoothed using Savitzky-Golay filtering with window size of 7. SAC-NF consistently shows earlier convergence and, on most tasks, better performance than the SAC baseline.

of normalizing flows of arbitrary length. The high expressivity of the later allows to (1) quickly discover richer policies (2) compress the cumbersome Gaussian policy into a lighter network and (3) better avoid local optima. Our proposed algorithm leverages connections between maximum entropy reinforcement learning and the evidence lower bound used to optimize variational approximations; this relationship allows for a straightforward extension of SAC to a wider class of distributions. We demonstrated through experiments on five MuJoCo environments that our method has a better convergence rate than the baseline, vastly improves the coverage of the parameter space and is at least as performant as SAC.

Acknowledgements

We want to thank Compute Canada/Calcul Québec and Mila – Quebec AI Institute for providing computational resources. We also thank Chin-Wei Huang for insightful discussions.

References

- Aytar, Y.; Pfaff, T.; Budden, D.; Paine, T. L.; Wang, Z.; and de Freitas, N. 2018. Playing hard exploration games by watching youtube. *Advances in Neural Information Processing Systems*.
- Bellemare, M. G.; Srinivasan, S.; Ostrovski, G.; Schaul, T.; Saxton, D.; and Munos, R. 2016. Unifying count-based exploration and intrinsic motivation. *Advances in Neural Information Processing Systems*.
- Bellemare, M. G.; Dabney, W.; and Munos, R. 2017. A distributional perspective on reinforcement learning. *International Conference on Machine Learning*.
- Bellman, R. 1957. A markovian decision process. *Journal of Mathematics and Mechanics* 679–684.
- Conti, E.; Madhavan, V.; Such, F. P.; Lehman, J.; Stanley, K. O.; and Clune, J. 2017. Improving exploration in evolution strategies for deep reinforcement learning via a population of novelty-seeking agents. *Advances in Neural Information Processing Systems*.
- Doan, T.; Mazouze, B.; and Lyle, C. 2018. Gan q-learning. *arXiv preprint arXiv:1805.04874*.
- Ecoffet, A.; Huizinga, J.; Lehman, J.; Stanley, K. O.; and Clune, J. 2019. Go-explore: a new approach for hard-exploration problems. *arXiv preprint arXiv:1901.10995*.
- Fujimoto, S.; van Hoof, H.; and Meger, D. 2018. Addressing function approximation error in actor-critic methods. *International Conference on Machine Learning*.
- Gal, Y., and Ghahramani, Z. 2016. Dropout as a bayesian approximation: Representing model uncertainty in deep learning. In *International Conference on Machine Learning*, 1050–1059.
- Goodfellow, I.; Pouget-Abadie, J.; Mirza, M.; Xu, B.; Warde-Farley, D.; Ozair, S.; Courville, A.; and Bengio, Y. 2014. Generative adversarial nets. In *Advances in Neural Information Processing Systems*, 2672–2680.
- Haarnoja, T.; Tang, H.; Abbeel, P.; and Levine, S. 2017. Reinforcement learning with deep energy-based policies. *CoRR* abs/1702.08165.
- Haarnoja, T.; Zhou, A.; Abbeel, P.; and Levine, S. 2018. Soft actor-critic: Off-policy maximum entropy deep reinforcement learning with a stochastic actor. *International Conference on Machine Learning*.
- Henderson, P.; Doan, T.; Islam, R.; and Meger, D. 2017. Bayesian policy gradients via alpha divergence dropout inference. *NIPS Bayesian Deep Learning Workshop*.
- Huang, C.; Krueger, D.; Lacoste, A.; and Courville, A. C. 2018. Neural autoregressive flows. *International Conference on Machine Learning*.
- Kingma, D. P., and Ba, J. 2015. Adam: A method for stochastic optimization. *International Conference on Learning Representations*.
- Kingma, D. P., and Welling, M. 2014. Auto-encoding variational bayes. *International Conference on Learning Representations*.
- Kingma, D. P.; Salimans, T.; and Welling, M. 2016. Improving variational inference with inverse autoregressive flow. *Advances in Neural Information Processing Systems*.
- Lillicrap, T. P.; Hunt, J. J.; Pritzel, A.; Heess, N.; Erez, T.; Tassa, Y.; Silver, D.; and Wierstra, D. 2016. Continuous control with deep reinforcement learning. In *4th International Conference on Learning Representations, ICLR 2016, San Juan, Puerto Rico, May 2-4, 2016, Conference Track Proceedings*.
- Maaten, L. v. d., and Hinton, G. 2008. Visualizing data using t-sne. *Journal of Machine Learning Research* 9(Nov):2579–2605.
- Mnih, V.; Badia, A. P.; Mirza, M.; Graves, A.; Lillicrap, T. P.; Harley, T.; Silver, D.; and Kavukcuoglu, K. 2016. Asynchronous methods for deep reinforcement learning. *CoRR* abs/1602.01783.
- Osband, I.; Blundell, C.; Pritzel, A.; and Roy, B. V. 2016. Deep exploration via bootstrapped DQN. *Advances in Neural Information Processing Systems*.
- Pathak, D.; Agrawal, P.; Efros, A. A.; and Darrell, T. 2017. Curiosity-driven exploration by self-supervised prediction. *International Conference on Machine Learning*.
- Puterman, M. L. 2014. *Markov decision processes: discrete stochastic dynamic programming*. John Wiley & Sons.
- Rezende, D. J., and Mohamed, S. 2015. Variational inference with normalizing flows. *International Conference on Machine Learning*.
- Schulman, J.; Levine, S.; Moritz, P.; Jordan, M. I.; and Abbeel, P. 2015. Trust region policy optimization.
- Sutton, R. S.; McAllester, D.; Singh, S.; and Mansour, Y. 1999. Policy gradient methods for reinforcement learning with function approximation. In *Proceedings of the 12th International Conference on Neural Information Processing Systems, NIPS'99*, 1057–1063. Cambridge, MA, USA: MIT Press.
- Tang, Y., and Agrawal, S. 2018. Boosting trust region policy optimization by normalizing flows policy.
- Tang, H.; Houthoof, R.; Foote, D.; Stooke, A.; Chen, X.; Duan, Y.; Schulman, J.; Turck, F. D.; and Abbeel, P. 2016. #exploration: A study of count-based exploration for deep reinforcement learning. *Advances in Neural Information Processing Systems*.
- Todorov, E.; Erez, T.; and Tassa, Y. 2012. Mujoco: A physics engine for model-based control. In *Intelligent Robots and Systems (IROS), 2012 IEEE/RSJ International Conference on*, 5026–5033. IEEE.
- Tomczak, J. M., and Welling, M. 2016. Improving variational auto-encoders using householder flow. *NIPS Bayesian Deep Learning Workshop*.

Supplementary Material

Experimental parameters

We provide a table of hyperparameters used to obtain results in the MuJoCo domain. Note that h^1 corresponds to the concatenated, h^2 to the average and h^3 to the conditional models.

NF parameters				
	# flows	type	alpha	model
Ant-v2	3	radial	0.05	conditional
HalfCheetah-v2	4	radial	0.05	concat
Hopper-v2	5	radial	0.05	conditional
Humanoid-v2	4	radial	0.05	average
Walker-v2	4	radial	0.05	average

Adam Optimizer parameters	
α_γ	3.10^{-4}
α_ω	3.10^{-4}
α_θ	3.10^{-4}
α_ϕ	3.10^{-4}

Algorithm parameters	
m	256
\mathcal{B} size	10^6

Table 2: SAC-NF parameters.

Comparing visitation states

In this part, we highlight the advantage of augmenting any simple policy with normalizing flows. For that purpose, we compared the state visitation counts of SAC-NF and SAC for `Humanoid-v2`. This is a challenging task which is known to require a high amount of exploration to avoid deceptively falling in a suboptimal solution. In Figure 5, we ran 15 rollouts for each methods (keeping the noise on) and projected the states visited in a two-dimensional dimension (with t -SNE (Maaten and Hinton, 2008)). NF expressivity allows our method to visit more diverse states and hence converge to good policies earlier. The major downside of the Gaussian policy lies in its symmetric nature, which prevents it from arbitrary focusing on subsets of the action space.

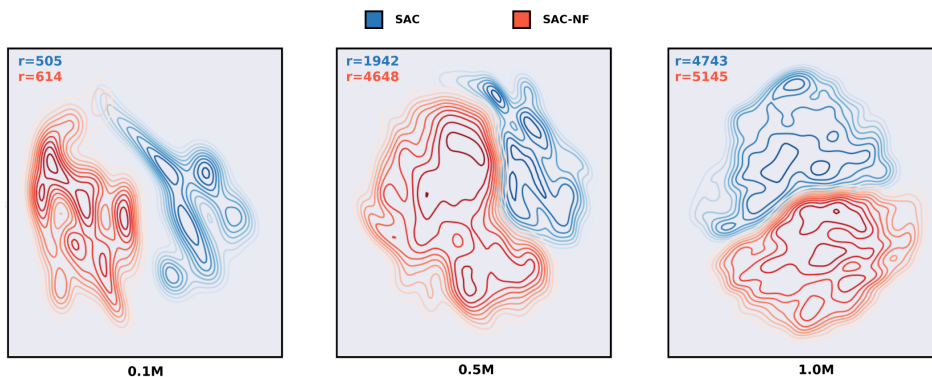


Figure 5: t -SNE of the state visitation for SAC and SAC-NF on `Humanoid-v2` over 100k, 500k and 1 million timesteps. Normalizing flow layers allow for better exploration, helping SAC-NF converge faster to high reward policies. The top left values indicates the average reward over 15 rollouts for each method; the bottom values indicate training steps.